CHEMICAL ENGINEERING TRANSACTIONS
VOL. 81, 2020
A publication of AIDIC
The Italian Association of Chemical Engineering
Online at www.cetjournal.it
Guest Editors: Petar S. Varbanov, Qiuwang Wang, Min Zeng, Panos Seferlis, Ting Ma, Jiří J. Klemeš

**ISBN** 978-88-95608-79-2; **ISSN** 2283-9216
DOI: 10.3303/CET2081118

# A New Approach for Open-Cell Foam Topology Generation: A Case Study Involving Transpiration Cooling

Zhilong Cheng, Ruina Xu, Peixue Jiang*

Key Laboratory for Thermal Science and Power Engineering, Ministry of Education, Department of Energy and Power Engineering, Tsinghua University, Beijing 100084, China
jiangpx@tsinghua.edu.cn

Open-cell foam has extensive applications including the transpiration cooling, the porous media combustion, the solid oxide fuel cell, the phase change materials for energy storage and the artificial bone tissue. However, the topology construction of open-cell foam with controlled profiles (i.e. porosity and pore diameter) is of great challenge for the available techniques. There is an urgent need to develop a new topology generation approach of open-cell foam for maximizing the working performance and minimizing the negative impacts in the fields as mentioned above. In this paper, a new method based on the periodic level surface was proposed to build the open-cell foam topology according to the inputting pore profiles. A framework, consisting of the solid matrix-pore interface type selection module, the geometry and pore parameters inputting module, the characteristic parameters of the interface equation calculation module, and the topology simplification and optimization module, was built for the generation of open-cell foam. With the generated topology, pore-scale modelling of transpiration cooling in a T-junction was carried out. A case with uniform pore topology was conducted to analyze the wall temperature and transpiration cooling efficiency.

## 1. Introduction

Transpiration cooling is a more effective thermal protection technology in the aerospace engineering field in comparison with the convection cooling and film cooling thanks to its high cooling capacity, low coolant consumption, compact structure and flexible control (Xiong et al., 2014). Porous media acts as an important heat transfer carrier in the transpiration cooling system. Porous media has a long application list, including the transpiration cooling (Liu et al., 2010), the solid oxide fuel cell (Fu et al., 2020), the solar collector (Wang et al., 2017), the electronic cooling (Ghahremannezhad and Vafai, 2018) and the high-density energy storage (Apicella et al., 2019). The common porous media in the transpiration cooling system includes the platelet structure, the sintered metal foam and the ceramic matrix composite materials.

Topology optimization of open-cell foam used in the transpiration cooling is of great importance to its cooling performance. For example, pore gradation (Wu et al., 2018) was promising to enable high cooling efficiency under non-uniform heat load and eliminate temperature oscillations in the transpiration cooling with phase change. Combining the flexible open-cell foam design and the additive manufacture technology would be an attractive approach to satisfy the above requirements. Currently, the minimum printable pore diameter is about 50 - 200 μm depending on the material types. The latest work in Lawrence Livermore National Laboratory (Saha et al., 2019) indicated that the high-throughput fabrication was realizable for complex porous structure with micropores. However, one of the greatest challenges for the available transpiration cooling technique was how to construct the open-cell foam with accurate geometrical parameters and varied pore topology. The available open-cell foam design approaches include the Kelvin cell (Rickenbach et al., 2014), the Weaire-Phelan structure (Yao et al., 2018) and the triply periodic surfaces (Gabbrielli et al., 2013). The triply periodic surfaces method provided a mathematical manner to construct the interface of the pores and the solid matrix, which was promising to control the pore topology quantitatively. However, there are few available mathematical models to design the open-cell foam with controlled profiles (i.e. porosity and pore diameter). The major effort should be focused on filling the gap between the characteristic parameters in the triply periodic surface equation and the geometrical parameters of the open-cell foam.

Paper Received: 16/04/2020; Revised: 12/06/2020; Accepted: 17/06/2020
Please cite this article as: Cheng Z., Xu R., Jiang P., 2020, A New Approach for Open-Cell Foam Topology Generation: A Case Study Involving Transpiration Cooling, Chemical Engineering Transactions, 81, 703-708 DOI:10.3303/CET2081118

In this paper, a new mathematical model for constructing the open-cell foam topology will be developed based on the triply periodic surface. With the developed model, the characteristic parameters in the triply periodic surface equation and the geometrical parameters of open-cell foam are connected, providing a novel and practical manner to design the open-cell foam topology with uniform porosity and pore size. Thus, a typical transpiration cooling carrier can be obtained for numerical simulation. A pore-scale computational model of the transpiration cooling is established and verified through experimental data. Finally, a case study is implemented to analyze the flow and heat transfer in the transpiration cooling process.

## 2. Mathematically-defined open-cell foam topology

In this study, the implicit triply periodic surfaces method, as expressed in Eq(1), was investigated to generate the geometry of the open-cell foam. This method used a set of triply periodic level surfaces to produce skeletal graphs with different inter-connectivity orders. In this work, primitive (P) surface (order 6) was selected to approximate porous media, as expressed in Eq(2). $F(x, y, z) = 0$ was the interface of the solid matrix, and the pores, $F(x, y, z) < 0$ represented the solid matrix, and $F(x, y, z) > 0$ represented the pores. Two parameters $p$ and $q$ were introduced into Eq(2). A MATLAB script was developed to figure out the relation between $p/q$ and real porosity/pore diameter of the open-cell foam. Porosity ($\varepsilon$) was calculated by Eq(3). Monte Carlo method was employed to calculate the porosity in the MATLAB script. A large number of particles were randomly thrown in the computational domain, as indicated in Figure 1. Porosity was the ratio of red particle number over total particle number. Pore was assumed as a sphere; thus, the pore diameter ($d_p$) was defined as Eq(4).

$$F(x,y,z) = 1 + \sum_{c=1}^{d} a_c \sin^i x \cdot \sin^j y \cdot \sin^k z \cdot \cos^l x \cdot \cos^m y \cdot \cos^n z = 0, i, j, k, l, m, n = 0, 1 \quad (1)$$

$$F(x,y,z) = 10(\cos(px) + \cos(py) + \cos(pz)) - 5.1(\cos(px)\cdot\cos(py) + \cos(py)\cdot\cos(pz) + \cos(pz)\cdot\cos(px)) + q \quad (2)$$

$$\varepsilon = V_{F(x,y,z)>0} / (V_{F(x,y,z)<0} + V_{F(x,y,z)>0}) \quad (3)$$

$$d_p = 2\left(\frac{3 \cdot V_{total} \cdot \varepsilon}{4\pi \cdot N_{pore}}\right)^{1/3} \quad (4)$$

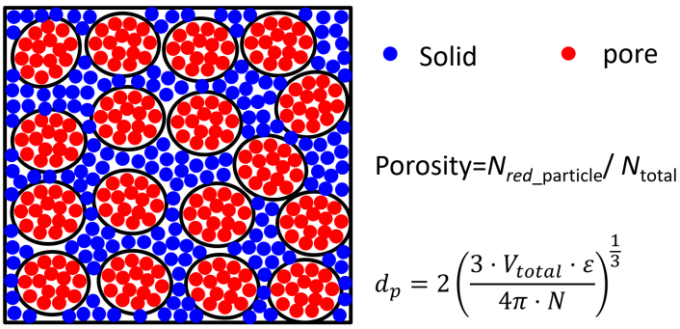


*Figure 1: Monte Carlo method for porosity and pore diameter calculations*

Pore topology in open-cell foam is usually defined by porosity, pore diameter and other parameters. The effects of $p$ and $q$ on porosity and pore diameter were examined. The computational domain was 8π × 8π × 8π, the particle number was 1,000,000 × 1,000,000 × 1,000,000. The impacts of $p$ and $q$ on porosity are shown in Figure 2. It was evident that $q$ had a significant impact on porosity. However, the influence of $p$ on porosity was insignificant. Thus, $q$ could be regarded as the porosity controller in this work. Figure 3 indicated that the pore diameter was controlled by $p$, as well as $q$.

With the given Eq(2), the topology of open-cell foam with predefined porosity and pore diameter can be obtained by calculating the $p$ and $q$. Firstly, A MATLAB script was developed to calculate $p$ and $q$ in Eq(2) depending on the inputting porosity and pore diameter. Secondly, according to the computed $p$ and $q$, the open-cell foam topology was generated in a software package (MathMod). Thirdly, the topology was modified (i.e. clean / repair, simplification and smooth). Finally, the topology was imported into a CFD software for numerical simulation or

into additive manufacture system. The local pore size at different slices in the type P unit was also calculated, as shown in Figure 4a. It was also noted that the ratios of the minimum pore size over the equivalent pore size and the maximum pore size over the equivalent pore size were fixed values at various *p*, as shown in Figure 4b.

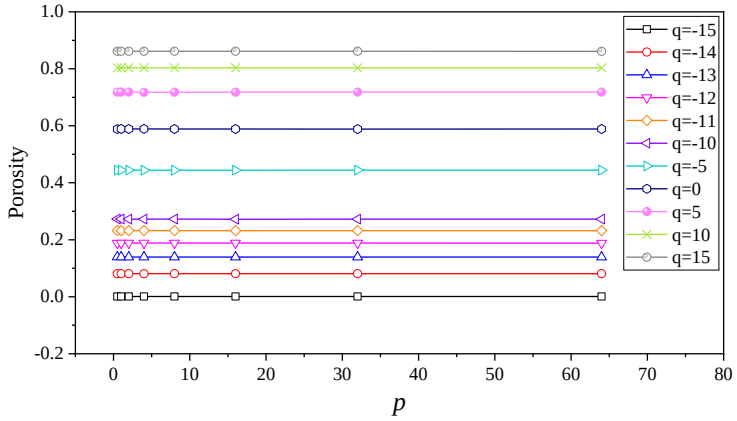


*Figure 2: Impacts of p and q on porosity*

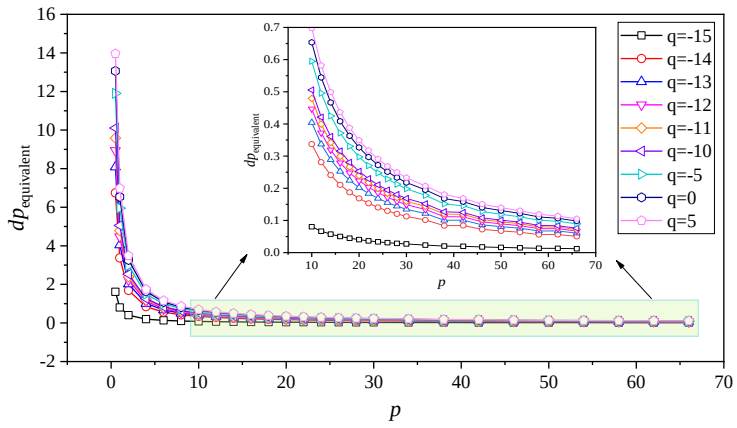


*Figure 3: Impacts of p and q on pore diameter*

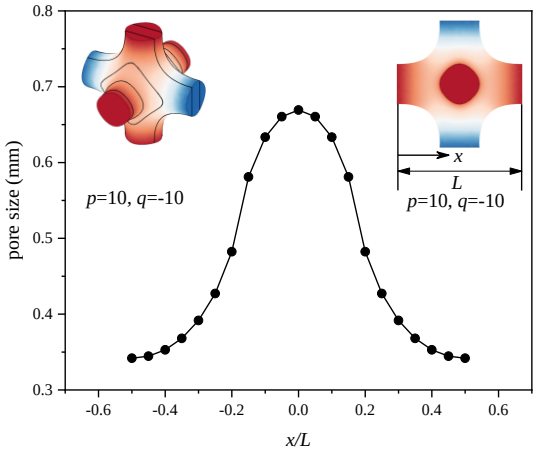


(a) Local pore diameter

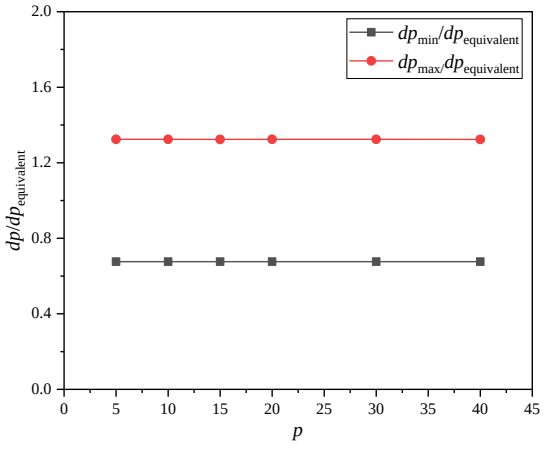


(b) $d_{p,\,max}/d_{p,\,equivalent}$ and $d_{p,\,min}/d_{p,\,equivalent}$

*Figure 4: Pore diameter characteristics of Type P*

## 3. A case study: Pore-scale simulation of transpiration cooling

In this section, a numerical case study for transpiration cooling was implemented to analyze the flow and heat transfer performances of the new open-cell foam topology. Prior to the discussion of the simulation results, the topology generation of porous transpiration carrier and the simulation methods were presented in Section 3.1 and Section 3.2.

### 3.1 Topology generation of porous transpiration carrier

With the open-cell foam topology construction method, the transpiration cooling carrier was built. The specified parameters were presented in Table 1. Beyond that, a porous plate with straight holes was also created for the model validation with the experimental data. The holes configuration was kept the same as the experimental sample (Huang et al., 2018)

*Table 1: Parameter specifications of the open-cell foam in the case study*

| Unit type | Porosity | Equivalent pore size | *p value* | *q value* |
|---|---|---|---|---|
| Primitive type | 0.1563 | 0.25 mm | 16.80 | -12.67 |

### 3.2 Pore-scale simulation method

Transpiration cooling involves the fluid flow and fluid-solid conjugate heat transfer. The computational domain is presented in Figure 5a. The mesh refinement was implemented in the interaction region between the main flow zone and open-cell foam zone. In the main flow channel, hot air passed over the target surface. Coolant flowed through the open-cell foam where the intensive heat transfer occurred. After flowing out the open-cell foam, air formed a thin film on the target surface with high heat flux (Huang et al., 2018), as indicated in Figure 5b. The governing equations include continuity, momentum and energy equations for the fluid zone and energy equation for the solid zone. The boundary conditions were given below:

- At the main flow inlet: $V_{air,\,in}$ = 11 m/s, $T_{air,\,in}$ = 340 K;
- At the coolant inlet: blow ratio ($V_c\rho_c$) / ($V_{air,\,in}\rho_{air,\,in}$) = 1 %, $T_c$ = 296 K;
- At the interface of pore and solid matrix: no-slip and coupled wall;
- At the outlet: pressure outlet.

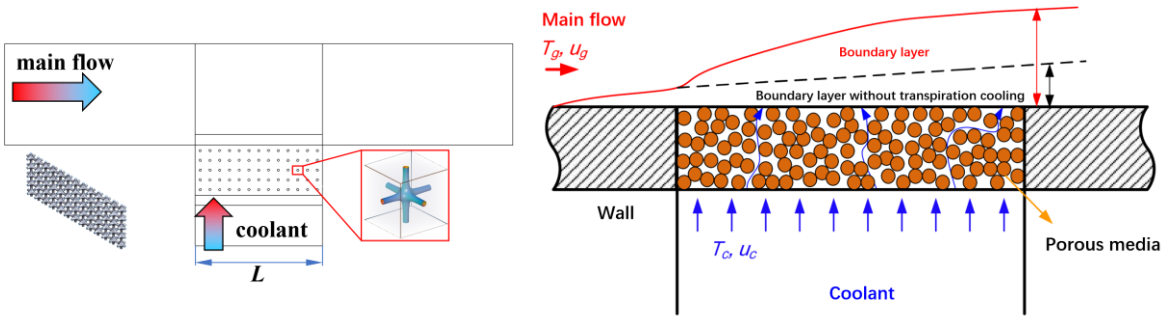


(a) Computational model (b) Illustration of transpiration cooling (Huang, 2015)

*Figure 5: Computational setup*

The Navier–Stokes and energy equations were solved using the ANSYS FLUENT 16.0. The pressure-velocity coupling method was the semi-implicit method for pressure linked equations (SIMPLE). The discrete scheme of pressure equation was standard. The discretization schemes of momentum and energy equations were power law. The main flow and coolant were air whose velocities and temperatures were specified in the boundary conditions. The thermophysical properties of air were dependent on temperature. The hybrid mesh (structured and unstructured) was adopted.

### 3.3 Results and discussion

The computational model validation was implemented by comparing the calculated results with the available experimental data (Huang et al., 2018), as shown in Figure 6a. The computational domain was completely same with the experimental configuration. It was observed that the *k-ω* turbulence model was more suitable than the SST and *k-ε* models. The maximum relative error of cooling efficiency ($\eta = (T_{air,\,in}-T_w) / (T_{air,\,in}-T_{coolant,\,in})$) between the calculated result and the experimental data was approximately 10.7 %. The error was mainly attributed from

the pore shrinkage during the sample fabrication process by selective laser melting additive manufacturing technology. The design pore size was 0.3 mm. However, the actual pore size was around 0.25 mm adhering with metal particles on the pore surfaces. Generally, the accuracy of the computational model was acceptable. The temperature contour was presented in Figure 6b.

Due to the limitation of computational resource, the employed open-cell foam in the case study (Type P) was much smaller than the size of the experimental sample with straight holes. The length of the experimental open-cell foam sample was 30 mm. The length of the open-cell foam in the case study was 13 typical units (~5 mm). The cooling efficiencies in the open-cell foam (Type P) and the porous media with straight holes were shown in Figure 6c. It was observed that the transpiration cooling efficiency in the Type P open-cell foam was higher due to the larger specific surface area. The temperature contour was presented in Figure 6d.

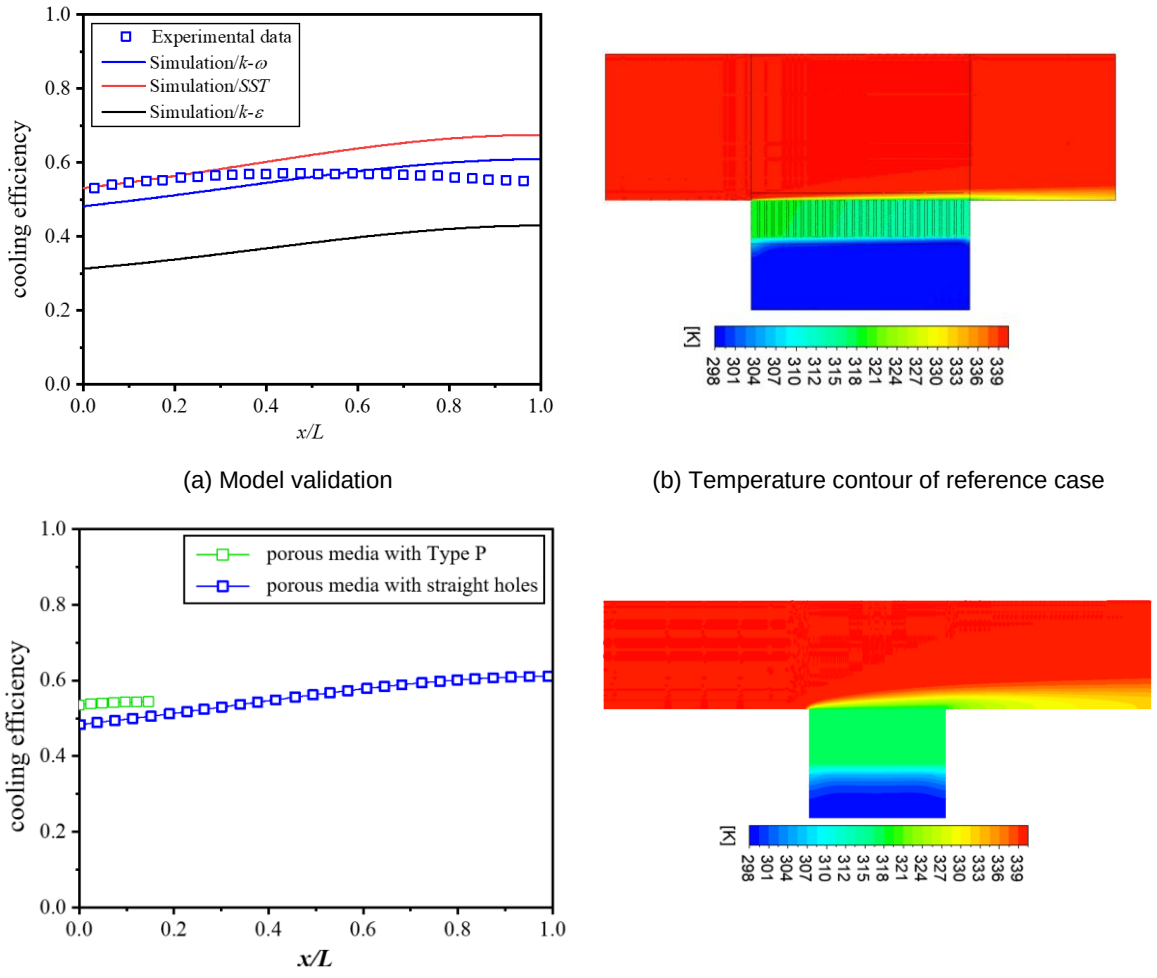


(a) Model validation

(b) Temperature contour of reference case

(c) Comparison of Type P and reference case

(d) Temperature contour of Type P

*Figure 6: Computational results*

## 4. Conclusions

Aiming at maximizing the cooling efficiency and minimizing the negative impacts in the transpiration cooling system, topology optimization of open-cell foam is of great importance. In this paper, a new open-cell foam topology construction approach with flexible controls of porosity and pore size was developed by connecting the actual porosity and pore size with the characteristic parameters in the triply periodic equations. With the approach as mentioned above, a typical transpiration cooling carrier (porosity: 0.1563, equivalent pore size: 0.25 mm) was built for pore-scale numerical simulation. Through computations, it was observed that the cooling efficiency and the film layer thickness of Type P geometry were larger than those of the straight-hole porous media. The parametric studies and experiments with different pore distributions (constant and smoothly graded

pore topology) are ongoing to reveal the flow and heat transfer behaviours further and achieve higher transpiration cooling performance.

**Acknowledgements**

We would like to acknowledge financial supports for this work provided by the China Postdoctoral Science Foundation (No. 2019M660036).

## References

Apicella B., Russo C., Di Blasi A., Mennella V., Antonucci V., Senneca O., Cerciello F., Ciajolo A., 2019, Nano-restructuration of carbon materials under high temperature heat treatment for environmental application and energy storage, Chemical Engineering Transactions, 73, 91-96.

Fu P., Yang J., Wang Q.W., 2020, Numerical study on mass transfer and electrical performance of anode-supported planar solid oxide fuel cells with gradient porosity anode, Journal of Heat Transfer, 142, 022101.

Gabbrielli R., Turner I.G., Bowen C.R., 2013, Development of modelling methods for materials to be used as bone substitutes, Key Engineering Materials, 361-363, 903-906.

Ghahremannezhad A., Vafai K., 2018, Thermal and hydraulic performance enhancement of microchannel heat sinks utilizing porous substrates, International Journal of Heat and Mass Transfer, 122, 1313-1326.

Huang G., Min Z., Yang L., Jiang P.X., Chyu M., 2018, Transpiration cooling for additive manufactured porous plates with partition walls, International Journal of Heat and Mass Transfer, 124, 1076-1087.

Huang Z., 2015, Transpiration cooling in supersonic and high temperature flow, PhD Thesis, Tsinghua University Department of Energy and Power, Beijing, China.

Liu Y.Q., Jiang P.X., Jin S.S., Sun J.G., 2010, Transpiration cooling of a nose cone by various foreign gases, International Journal of Heat and Mass Transfer, 53, 5364-5372.

Rickenbach J.V., Lucci F., Narayanan C., Eggenschwiler P.D., Poulikakos D., 2014, Multi-scale modelling of mass transfer limited heterogeneous reactions in open-cell foams, International Journal of Heat and Mass Transfer, 75, 337–346.

Saha S.K., Wang D., Nguyen V.H., Chang Y., Oakdale J.S., Chen S.C., 2019, Scalable submicrometer additive manufacturing, Science, 366, 105-109.

Wang P., Li J.B., Bai F.W., Liu D.Y., Xu C., Zhao L., Wang Z.F., 2017, Experimental and theoretical evaluation on the thermal performance of a windowed volumetric receiver, Energy, 119, 652-661.

Wu N., Wang J.H., He F., Chen L., Ai B.C., 2018, Optimization transpiration cooling of nose cone with non-uniform permeability, International Journal of Heat and Mass Transfer, 127, 882-891.

Xiong Y.B., Zhu Y.H., Jiang P.X., 2014, Numerical simulation of transpiration cooling for sintered metal porous strut of the scramjet combustion chamber, Heat Transfer Engineering, 35, 4-6.

Yao Y.P., Wu H.Y., Liu Z.Y., 2018, Direct simulation of interstitial heat transfer coefficient between paraffin and high porosity open-cell metal foam, Journal of Heat Transfer, 140, 032601.